ELSEVIER

Nuclear Instruments and Methods in Physics Research A 364 (1995) 380–393

NUCLEAR INSTRUMENTS & METHODS IN PHYSICS RESEARCH Section A

A statistical technique for characterizing X-ray position-sensitive detectors

E. Dufresne [a,*], R. Brüning [a], M. Sutton [a], B. Rodricks [b], G.B. Stephenson [c]

[a] Centre for the Physics of Materials, Department of Physics, McGill University, Montreal, QC, H3A 2T8, Canada
[b] Advanced Photon Source, Argonne National Laboratory, 9700 South Cross Avenue, Argonne, IL 60439, USA
[c] IBM Research Division, Thomas J. Watson Research Center, Yorktown Heights, NY 10598, USA

Received 9 February 1995

Abstract

We present a technique for characterizing X-ray sensitive photodiode arrays and charge-coupled device (CCD) arrays. The technique uses simple statistical estimators (means, variances and correlation functions) to determine the response, noise, resolution and detective quantum efficiency of a position-sensitive detector. We apply this technique by characterizing a linear diode array and a CCD array exposed to direct illumination by X-rays. Correlations between neighboring pixels were important, and they are included in the calculation of the detective quantum efficiency and noise of the detector.

1. Introduction

The advent of high intensity X-ray synchrotron sources coupled with the development of X-ray position-sensitive detectors (PSD) has allowed us to study time-resolved non-equilibrium dynamics in solid-state systems. For example, one-dimensional PSD have been used to study the isothermal crystallization of metallic glasses by measuring structure factors with a time resolution of a few milliseconds [1], and to study the early stage dynamics of order-disorder transitions in Fe_3Al [2] and Cu_3Au [3]. Two-dimensional PSD have been used to study the dynamics of a first order phase transition in Cu_3Au with coherent X-rays [4] and to determine strain kinetics in $In_xGa_{1-x}As$ quantum wells [5].

To obtain meaningful quantitative data from a PSD, one must know whether the response of the detector is linear with respect to the number of incident photons, measure the uniformity of response over the detector area, and determine the noise, the resolution function, and the detective quantum efficiency. For coherent diffraction experiments [4], the full spatial resolution of the detector is required, and spatial and temporal correlation of the signal are the quantities to be measured. Thus correlations inherent to the detector have to be exactly known.

In this paper, we show how the response of a PSD can be characterized by comparing measured averages, variances and pixel-to-pixel correlation functions to the expected statistical estimators for Poisson counting statistics. Similar techniques have been used previously to measure the detective quantum efficiency of a detector [6], or to evaluate the linearity constant between the PSD signal and the number of detected photons [7]. Significant spatial correlation exists between neighboring pixels for a typical PSD (see Figs. 2 and 10). We show how to extract the resolution from the measured correlation function. The effect of a finite detector resolution, which induces spatial correlations between neighboring pixels of a PSD, reduces the noise of the PSD when compared to expected Poisson noise. This must be taken into account in the evaluation of the detective quantum efficiency.

In Section 2, we first discuss the case where each pixel of the detector is independent of its neighbors. Then, we generalize this technique to include the spatial correlation that may be present in a real one- or two-dimensional detector. Finally, two examples are given: Section 3 gives the characterization of a X-ray sensitive linear photodiode array, and Section 4 describes a more general treatment for a two-dimensional charge coupled device (CCD).

2. Description of the technique

2.1. Description of the detection process.

Solid-state PSD are typically made of an array of Si photodiodes or MOS capacitors, which can be used as integrating detectors for X-rays. Two modes of operation of solid-state X-ray detectors are generally used: direct X-ray illumination or optical coupling using light produced in an X-

* Corresponding author. Tel.: +1 514 398 7033; Fax: +1 514 398 6526; E-mail: eric@physics.mcgill.ca.

0168-9002/95/$09.50 © 1995 Elsevier Science B.V. All rights reserved
SSDI 0168-9002(95)00335-5

Table 1
Definitions

τ	Exposure time
$V(\boldsymbol{r},t)$	Digital signal measured at position $\boldsymbol{r}=\boldsymbol{r}_{ij}$ between time t_k and $t_k+\tau$. $\boldsymbol{r}_{ij}$ and t_k are discrete due to the nature of the detection process
$n_i(\boldsymbol{r},t)$	Incident number of photons on the surface of a pixel $\boldsymbol{r}$ at t as measured by a reference detector having near unit detective quantum efficiency
$n_d(\boldsymbol{r},t)$	Detected number of photons.
$\alpha=\frac{\langle n_d\rangle_t}{\langle n_i\rangle_t}$	Detective quantum efficiency of the detector
$\langle V(\boldsymbol{r},t)\rangle_t=\frac{1}{N}\sum_{i=1}^{N}V(\boldsymbol{r},t_i)$	Time average of signal V. It is measured by averaging a time sequence of N scans
$S^2_{t,V}(\boldsymbol{r})=\frac{1}{N-1}\sum_{i=1}^{N}(V(\boldsymbol{r},t_i)-\langle V(\boldsymbol{r},t)\rangle_t)^2$	Estimator for the variance of V, measured with a time sequence of N scans
$\langle V(\boldsymbol{r},t)\rangle_{\boldsymbol{r}}=\frac{1}{N_p}\sum_{i=1}^{N_p}V(\boldsymbol{r}_i,t)$	Spatial average of signal V. It is measured by averaging N_p pixels in a given scan at time t
$S^2_{\boldsymbol{r},V}(t)=\frac{1}{N_p-1}\sum_{i=1}^{N_p}(V(\boldsymbol{r}_i,t)-\langle V(\boldsymbol{r},t)\rangle_{\boldsymbol{r}})^2$	Estimator for the variance of N_p pixels

ray fluorescent material. Direct illumination of the detector gives the full spatial resolution of the pixels, while optical coupling increases the detective quantum efficiency for harder X-rays and allows for changes in the effective detector area by appropriate lenses. In this paper, we use direct illumination of the PSD. For silicon, 3.6 eV are required to create an electron–hole pair [8]. A photon in the range of 5–20 keV will generate thousands of electron–hole pairs, some of which are then collected on the Si diode capacitance. After a preset exposure time τ, the collected charge is measured, amplified, digitized and finally cleared for the next integration. The digitized signal $V(\boldsymbol{r},t)$ is an integer number measured in analog-to-digital units (ADU). Here $\boldsymbol{r}$ is a discrete one- or two-dimensional vector pointing to the center of a given pixel of the PSD, and t refers to the integration between time t and $t+\tau$. The variables used are summarized in Table 1. The number of ADU per detected photon is determined by the gain of the digitizer circuit. A so-called dark pattern must be taken without illumination to subtract an offset signal from the data, which may vary from pixel to pixel. To relate the detected signal to the incident intensity, one has to measure the detector linearity, uniformity, noise, resolution and detective quantum efficiency.

Illuminating the detector with a spatially uniform source of light or X-rays allows one to test the uniformity of the detector response. To generate this uniform source, we scatter a beam of monochromatic X-rays from an amorphous sample (e.g. a piece of polyimide [7,9] or polystyrene) and place the detector far away from the sample.

To test linearity, one varies the incident flux of photons and the integration time independently to see whether the number of photons incident on the surface of pixel $\boldsymbol{r}$, integrated between t and $t+\tau$, $n_i(\boldsymbol{r},t)$, is the only relevant quantity. One must find a function that relates the detected signal V to n_i so that $V=f(n_i)$. In general, f may not be linear. Therefore to linearize the detector's signal, one would apply the inverse of f to V. Details of this treatment are given in Section 4.

We assume that the noise in the signal V has two sources: counting statistics of the photons and an "electronic" noise from the detection process. Naturally, the noise due to counting statistics depends on n_d, the number of detected photons, rather than on n_i. In general $\langle n_d(\boldsymbol{r},t)\rangle_t=\alpha(\boldsymbol{r})\langle n_i(\boldsymbol{r},t)\rangle_t$, where $\alpha(\boldsymbol{r})$ is called the detective quantum efficiency of a pixel centered at $\boldsymbol{r}$, as defined in Ref. [6]. Here the brackets refer to a time average. One finds that $\alpha<1$ because photons are absorbed or reflected before they reach the detection volume, or because they pass the detection volume without detection. We show how $n_d(\boldsymbol{r},t)$ may be determined by analyzing the fluctuations in the signal $V(\boldsymbol{r},t)$ for equivalent exposures.

2.2. Technique for characterizing independent linear detectors

The detector characterization technique is based on the following idea. Due to the nature of the detection process, n_d obeys Poisson statistics, so the mean and variance of n_d are equal [10]. If we assume linearity and neglect any electronic noise contribution from the detector electronics, the signal in a detector is given by $V=kn_d$, where k is the calibration constant, equal to the average number of ADU per detected photons. By measuring N patterns, we can calculate the signal mean and variance from their definitions in Table 1. $\langle V\rangle_t=k\langle n_d\rangle_t$ is the mean signal. The variance of V, $S^2_{t,V}$, is equal to $k^2S^2_{t,n_d}$, and for Poisson noise, $S^2_{t,n_d}=\langle n_d\rangle_t$. So the ratio $S^2_{t,V}/\langle V\rangle_t=k$ allows to measure the calibration constant. Unless otherwise stated, the terms mean and

variance used in this paper refer to the unbiased estimators of the true mean and variance of a given variable. Here we assumed that the signal V in a given pixel is independent of the signal in its nearest neighbors, and that the standard deviation of the number of photo-electrons created per detected photons is much smaller than its average [7]. What follows is a generalization of this idea by considering other noise sources and couplings between detectors.

For a real PSD, we found that the ratio k increases as $\langle V\rangle_t$ approaches zero, due to electronic noise contributions to the variance. This intensity dependence can be removed by including in V the detected photons and the electronic noise contributions so that

$$V(\boldsymbol{r},t) = k(\boldsymbol{r})n_d(\boldsymbol{r},t) + V_e(\boldsymbol{r},t), \tag{1}$$

and on average

$$\langle V(\boldsymbol{r},t)\rangle_t = k(\boldsymbol{r})\langle n_d(\boldsymbol{r},t)\rangle_t. \tag{2}$$

Note that here the value of k may vary between different pixels. V_e is the electronic noise signal, and we assumed $\langle V_e\rangle_t \approx 0$, which is assured by the subtraction of the dark pattern described earlier. We assume both V_e and n_d are independent random variables. The physics of this noise is discussed in details elsewhere [6]. Here we are only interested on the mean and variance of the noise, which are measured separately with the source of X-rays turned off. The time averaged variance of $V(\boldsymbol{r},t)$ is

$$S^2_{t,V}(\boldsymbol{r}) = k^2(\boldsymbol{r})S^2_{t,n_d}(\boldsymbol{r}) + S^2_{t,V_e}(\boldsymbol{r}) + 2k(\boldsymbol{r})\,\mathrm{cov}_t(n_d(\boldsymbol{r},t), V_e(\boldsymbol{r},t)), \tag{3}$$

where

$$\mathrm{cov}_t(A,B) = \frac{1}{N-1}\sum_{i=1}^{N}(A(t_i) - \langle A\rangle_t)(B(t_i) - \langle B\rangle_t) \tag{4}$$

is the covariance of two random variables A and B. $\mathrm{cov}_t(n_d, V_e) \approx 0$, by the assumption of independence. Dividing Eq. (3) by Eq. (2), and recalling that $S^2_{t,n_d}(\boldsymbol{r}) = \langle n_d(\boldsymbol{r},t)\rangle_t$ for a Poisson distribution [10], one finds that

$$k(\boldsymbol{r}) = \frac{S^2_{t,V}(\boldsymbol{r}) - S^2_{t,V_e}(\boldsymbol{r})}{\langle V(\boldsymbol{r},t)\rangle_t}. \tag{5}$$

To determine an estimate of the ratio of ADU to detected photons for each pixel, one evaluates the mean and variance for each pixel based on N scans, subtracting a measured dark variance S^2_{t,V_e} from the signal variance. The subtraction of S^2_{t,V_e} in Eq. (5) makes k intensity independent for a real PSD, as the average signal goes to zero. Once $k(\boldsymbol{r})$ is known, $\alpha(\boldsymbol{r})$ can be calculated after measuring $n_i(\boldsymbol{r},t)$ with a detector with near unit efficiency. The detective quantum efficiency may then be calculated as

$$\alpha(\boldsymbol{r}) = \frac{\langle V(\boldsymbol{r},t)\rangle_t}{k(\boldsymbol{r})\langle n_i(\boldsymbol{r},t)\rangle_t}. \tag{6}$$

The spatial variations of the detector array appear as the variations in $k(\boldsymbol{r})$, or detector to detector variations. In order to determine whether these fluctuations are significant, the error in $k(\boldsymbol{r})$ expected from Poisson and electronic noise has to be considered. The uncertainty in the determination of $k(\boldsymbol{r})$ depends on the number of measurements N. From standard error propagation analysis (see the derivation in the Appendix), we estimate the expected error in k, $\sigma_k(\boldsymbol{r})$, by

$$\frac{\sigma_k^2(\boldsymbol{r})}{k^2(\boldsymbol{r})} \approx \frac{2}{N-1}\left(1 + \frac{S^4_{t,V_e}(\boldsymbol{r})}{k^2(\boldsymbol{r})\langle V(\boldsymbol{r},t)\rangle_t^2}\right) + \frac{S^2_{t,V_e}(\boldsymbol{r})}{\langle V(\boldsymbol{r},t)\rangle_t^2}\left(\frac{1}{N} + \frac{1}{N_d}\right). \tag{7}$$

Here, we used $S^2_{t,V} - S^2_{t,V_e} = k\langle V\rangle_t$ to simplify Eq. (A.25). N_d is the number of scans used to determine the average dark pattern. Eq. (7) is made of four terms: the first term $2/(N-1)$ is the error due to counting statistics (see Eq. (A.22)) and the last three terms containing $S^2_{t,Ve}$ and $S^4_{t,Ve}$ are due to the electronic noise.

To minimize the error, one should take N as large as possible to reduce the error due to counting statistics. This is achieved by taking a small exposure time τ. As τ and V approaches zero, the minimum error is reached when both noise contributions to σ_k are equal. For smaller τ, σ_k increases due to the electronic noise. As a rule of thumb, one should measure $N_d = N$ dark patterns, so that the average dark pattern is measured precisely. To get a relative precision $\epsilon = \sigma_k/k$, one should choose τ such that the detected signal $V \approx \sqrt{S^2_{t,V_e}\left\{1 + S^2_{t,V_e}/k^2\right\}}$, and measure $N \approx 4/\epsilon^2$ scans with and without X-rays.

For count rates available at synchrotron sources, one may find that the signal obtained for the finest time resolution τ is always much larger than the dark noise. Then fewer dark patterns need to be measured. For large signals $\langle V\rangle_t \gg \sqrt{S^2_{V_e}}$ and for $N \gg N_d$, $\sigma_k \approx k\sqrt{2/(N-1) + S^2_{V_e}/(N_d\langle V\rangle_t^2)}$. When $\langle V\rangle_t \gg V_m = \sqrt{S^2_{V_e}N/(2N_d)}$, $\sigma_k \approx k\sqrt{2/(N-1)}$, and counting statistics is the dominant contribution to the error. In Fig. 1b for example, the signal in the central pixels of the array is within this limit since $V_m = 66$ ADU. For $V < V_m$, σ_k is dominated by the detector electronic noise.

As mentioned above, this treatment assumed that each pixel is independent from its neighbors. If this is not true, this correlation reduces the variance, and $k(\boldsymbol{r})$ is not the number of ADU per detected photon. This case is discussed next.

2.3. Treatment including pixel-to-pixel correlations.

To understand the effect of couplings between detectors, we consider first a toy model for a one-dimensional PSD, where two neighboring pixels share some fraction x of their signals. Following the previous notation, replacing $\boldsymbol{r}$ by an integer index i, the signal in the ith pixel, $V(i,t)$, is defined by

$$V(i,t) = (1-x)kn_d(i,t) + xkn_d(i+1,t), \tag{8}$$

where k is the number of ADU per detected photon, and $n_d(i,t)$ is the number of photons measured by an independent detector if x was zero, and it is assumed that $0 \le x \le 0.5$. The case for $x \neq 0$ occurs in real PSD because the charge created by photons is shared by adjacent pixels. This coupling affects the statistics of the signal. For a spatially uniform exposure, $\langle n_d(i,t)\rangle_t$ and $\langle n_d(i+1,t)\rangle_t$ are the same within counting statistics, and $\langle V(i,t)\rangle_t$ equals on average $k\overline{n_d}$, where $\overline{n_d}$ is the mean of the probability density of n_d. For two independent Poisson distributed random variables [10], $n_d(i,t)$ and $n_d(i+1,t)$, with $\langle n_d(i,t)n_d(i+1,t)\rangle_t = \langle n_d(i,t)\rangle_t\langle n_d(i+1,t)\rangle_t = \overline{n_d}^2$, the variance of $V(i,t)$ is

$$\begin{aligned} S^2_{t,V}(i) &= \langle V(i,t)^2\rangle_t - \langle V(i,t)\rangle_t^2 \\ &= k^2\left\{(1-x)^2 + x^2\right\}\overline{n_d}. \end{aligned} \tag{9}$$

By letting $x = 0$, we recover the case discussed in Section 2.2. For a finite x, the variance is always smaller than the variance of uncoupled detectors as $(1-x)^2+x^2 \le 1$ for $0 \le x \le 0.5$. Now $S^2_{t,V}(i)/\langle V(i,t)\rangle_t = k\{(1-x)^2+x^2\}$, so that from a measurement of this ratio alone, k cannot be extracted. A second measurement is needed in order to solve for k and x.

The resolution function could be measured to determine x, by illuminating only one pixel with a source which is smaller than the pixel size. For a PSD, this requires collimating the X-ray beam through a pinhole with a diameter of only a few micrometers, and scanning the pinhole over the detector area. This technique may be difficult to apply, because one needs an intense X-ray source to generate a usable micrometer beam and a translation system with micrometer resolution. The measurements of pixel-to-pixel correlation offers a useful alternative for measuring the resolution function. In this model, the measured covariance of $V(i,t)$ and $V(i+1,t)$ is given by

$$\begin{aligned} &\mathrm{cov}_t(V(i,t), V(i+1,t)) \\ &= \langle V(i,t)V(i+1,t)\rangle_t - \langle V(i,t)\rangle_t\langle V(i+1,t)\rangle_t \\ &= x(1-x)k^2\overline{n_d}, \end{aligned} \tag{10}$$

which gives $k = (2\mathrm{cov}_t + S^2_{t,V})/\langle V\rangle_t$ and $x = \frac{1}{2} - 1/2\sqrt{(S^2_{t,V} - 2\mathrm{cov}_t)/(S^2_{t,V} + 2\mathrm{cov}_t)}$.

Next nearest neighbor pixels can also be coupled due to the diffusion of photo-electrons far away from the absorption site. To measure these distant correlations, a general correlation function between $V(\boldsymbol{r},t)$ and $V(\boldsymbol{r}+\boldsymbol{\Delta},t)$ is defined as

$$C(\boldsymbol{r},\boldsymbol{\Delta}) = \frac{\mathrm{cov}_t(V(\boldsymbol{r},t), V(\boldsymbol{r}+\boldsymbol{\Delta},t))}{\sqrt{S^2_{t,V}(\boldsymbol{r})S^2_{t,V}(\boldsymbol{r}+\boldsymbol{\Delta})}}, \tag{11}$$

where the averages and variances are defined in Table 1, and $\boldsymbol{\Delta}$ is the relative displacement between the pixels. Two limiting cases in this definition may be calculated easily. For large $\boldsymbol{\Delta}$, $V(\boldsymbol{r},t)$ and $V(\boldsymbol{r}+\boldsymbol{\Delta},t)$ are independent, and $C(\boldsymbol{r},\boldsymbol{\Delta}) = 0$. For $\boldsymbol{\Delta} = 0$, $C(\boldsymbol{r},0) = 1$ since the numerator becomes identical to $S^2_{t,V}$. If the signal between neighbors is not independent, one finds in general $-1 < C(\boldsymbol{r},\boldsymbol{\Delta}) < 1$.

To estimate the resolution function and its effect on the measured noise, we now include all pixel-to-pixel couplings. Developed for shot noise processes [11], the model describes a stochastic process created by random superposition of a constant response function $h(\boldsymbol{r}')$ for each photon [12]. The function $h(\boldsymbol{r}')$ describes the spread of the signal in the detector. The measured signal at pixel $\boldsymbol{r}$, $V(\boldsymbol{r},t)$, is a sum of disturbances which hit the detector at random positions $\boldsymbol{r}_i$,

$$V(\boldsymbol{r},t) = \sum_{i=1}^{n_d} h(\boldsymbol{r}_i - \boldsymbol{r}). \tag{12}$$

In our case, n_d is the number of detected photons between time t and $t+\tau$, sampled from a Poisson distribution. The $\boldsymbol{r}_i$ are chosen from a uniform distribution since the signal is assumed to be spatially uniform. The model can be generalized to include spatial variations in the incident signal [11], and the results will not depend on the fact that h may vary with each photon if the variance of h is small enough. The model further assumes that $h(\boldsymbol{r}')$ is the same for each pixel and that the signal in a given detector is not correlated in time. A complete derivation of the moments of V is given in detail in Ref. [11]. It is shown that

$$\langle V(\boldsymbol{r},t)\rangle_t = \langle n_d(\boldsymbol{r},t)\rangle_t 1/L^d \int h(\boldsymbol{r}')\,\mathrm{d}\boldsymbol{r}'^d, \tag{13}$$

$$\begin{aligned} S^2_{t,V} &= \langle V^2(\boldsymbol{r},t)\rangle_t - \langle V(\boldsymbol{r},t)\rangle_t^2 \\ &= \langle n_d(\boldsymbol{r},t)\rangle_t 1/L^d \int h^2(\boldsymbol{r}')\,\mathrm{d}\boldsymbol{r}'^d, \end{aligned} \tag{14}$$

$$\begin{aligned} C(\boldsymbol{r},\boldsymbol{\Delta}) &= \frac{\langle V(\boldsymbol{r},t)V(\boldsymbol{r}+\boldsymbol{\Delta},t)\rangle_t - \langle V(\boldsymbol{r},t)\rangle_t^2}{S^2_{t,V}} \\ &= \frac{\int h(\boldsymbol{r}')h(\boldsymbol{r}'+\boldsymbol{\Delta})\,\mathrm{d}\boldsymbol{r}'^d}{\int h^2(\boldsymbol{r}')\,\mathrm{d}\boldsymbol{r}'^d}, \end{aligned} \tag{15}$$

where L^d is the linear size or area of a detector in $d = 1,2$ dimensions. $\langle V(\boldsymbol{r},t)\rangle_t$, $S^2_{t,V}$ and $C(\boldsymbol{r},\boldsymbol{\Delta})$ can be estimated from repeated measurements, and $\langle n_d\rangle_t$ can be solved from these equations with an appropriate model for $h(\boldsymbol{r}')$. Choosing $h(\boldsymbol{r}') = k\delta(\boldsymbol{r}')$, we recover Eq. (5) from the ratio of Eqs. (14) and (13). Here, the model is further simplified by assuming that $h(\boldsymbol{r}')$ is discrete, and replacing integrals by sums. To recover Eqs. (9) and (10) from Eq. (13)–(15), let $h(0) = k(1-x)$, $h(1) = kx$, and $h(\boldsymbol{r}') = 0$, for $|\boldsymbol{r}'| > 1$. Using the measured spatial autocorrelation function, one can often evaluate the resolution function $h(\boldsymbol{r}')$

Table 2
Position-sensitive detectors characteristics

	EG&G Reticon 2048SAU-822	TI 4849 CCD
Array size	2048 pixels	390 by 584 pixels
Pixel dimension	25 μm wide, 2.0 mm high	22.4×22.4 μm
Specified resolution	1.5 pixels.	2 pixels
Characteristic length	Diffusion length 50 μm	Depletion layer 12 μm
Window	250 μm Be window, 1 μm SiO_2 overcoat	250 μm Be window
Amplifier gain	1 ADU/1300 electrons	Adjustable
Readout time	4 μs/pixel, 8 ms for the array	6 μs/pixel, 1 s for the array
Readout noise	< 1.2 ADU rms	20 electrons/pixel
Integration time	8 ms to two hours	A few μs to minutes

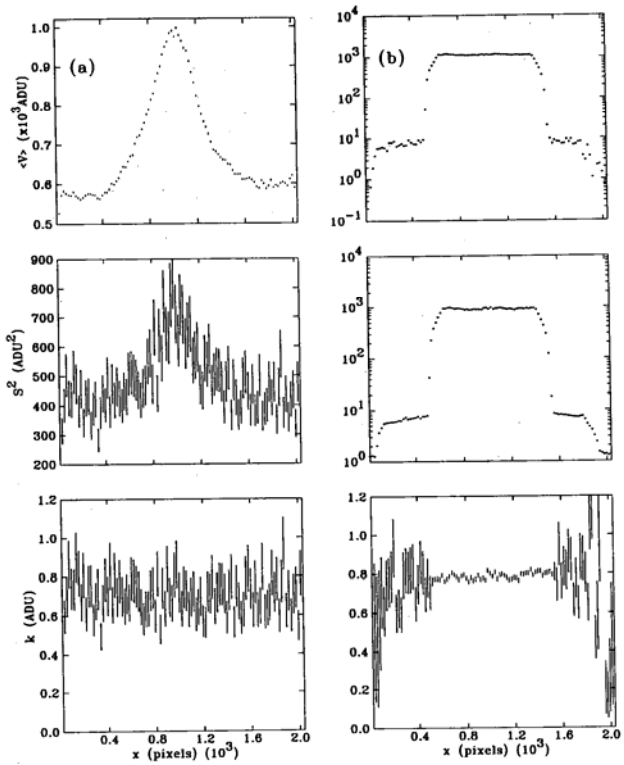

Fig. 1. (a) Time averaged signal $\langle V(r)\rangle_t$, variance $S^2_{t,V}(r)$, and calibration constant $k = S^2_{t,V}/\langle V(r)\rangle_t$ versus pixel number for 6.93 keV X-rays, $N = 100$. The error bars for the mean, variance and ratio are calculated from formulas discussed in Section 2 and the appendix. (b) Same as above, but with 8.05 keV X-rays, $N = 8000$.

by inverting Eq. (15). From Eq. (13), one can calculate n_d from $\langle V(\boldsymbol{r},t)\rangle_t$. Then Eq. (6) becomes

$$\alpha = \frac{L^d \langle V\rangle_t}{\langle n_i\rangle_t \int h(\boldsymbol{r}')\, \mathrm{d}\boldsymbol{r}'^d}. \tag{16}$$

Good statistics for the measured autocorrelation functions can be in principle obtained by correlating the signal from thousands of scans. If no time correlation exists and one expects the detectors to be almost identical, one can save this effort by taking a spatial average and variance over detectors of a single uniform scattering pattern instead of time averages. One can get excellent statistics from a single scan of a 500×500 CCD array by averaging over the 250 000 pixels. In the two examples discussed next, direct measurements showed no time correlation of the signals. For our detectors, we found that a time average and a spatial average are quantitatively similar, both for means and variances. Time averages or spatial averages can thus be interchanged for convenience.

3. Characterization of a linear PSD

The photodiode array used contains 2048 rectangular pixels with 25 μm wide and 2.0 mm high active areas. The resolution is specified as 1.5 pixels wide so there will be some correlation between pixels. It is operated at −40°C, cooled by a Peltier stage, to reduce the electronic noise. The array is operated by a Princeton Instrument ST1000 controller and the data is transferred to a IBM PC 386-AT through a custom designed I/O board from PI. Software is provided with the package to control the data acquisition parameters, store the data and visualize the data. Scans can be accumulated by a 32 bit register and pixels can be grouped to increase the scan rate while sacrificing the spatial resolution. Further characteristics of the detector are summarized in Table 2.

Fig. 1 shows some experimental data obtained for the linear array. As defined in Table 1 and Eq. (5), the mean, variance and ratio of variance over mean of V are plotted for every 20th pixels of the array at two different X-ray energies, 6.93 and 8.05 keV. The first data set was obtained by scattering 6.93 keV X-rays onto a Bragg peak of Fe_3Al, constant in time. 100 scattering patterns were averaged. Note that the mean is quite smooth (i.e. well defined to within 0.3%) but that the fluctuations on the variance are substantial (14%). For $N = 100$ measurements, the relative error on the mean is $1/\sqrt{Nn_d}$ with $n_d \approx 1000$, while the error on the variance is $\sqrt{2/(N-1)}$. The error bars on the ratio were calculated from Eq. (7). A least squares fit of $k(\boldsymbol{r})$ to a constant, weighted with error bars calculated from Eq. (7), yields $k = 0.682$ and a χ^2 of 1.1.

To determine the uniformity of $k(\boldsymbol{r})$, 8000 patterns were measured and analyzed. Fig. 1b was obtained by scattering 8.05 keV X-rays, coming from an X-ray tube with a Cu target and a Ge (111) monochromator set on Cu K_α. The beam covered approximately half of the array. The small tails on the average are due to diffuse scattering. Note the logarithmic axes for the mean and the variance; the signal varies over three order of magnitude but the ratio is essentially independent of signal level. A dark variance of 1.1 ADU^2 causes the large fluctuations in $k(\boldsymbol{r})$ when the X-ray signal is comparable to the electronic noise signal. Measuring more dark patterns (larger N_d) would reduce the error on k. A least-square fit of the ratio to a constant between pixel 650 to 1400 gives $k = 0.792$ and a χ^2 of 2, indicating the possibility of systematic variations in pixels with a rms amplitude of 2%. Note that a large number of identical exposures have to be analyzed to detect fluctuations this small. If signal variations between pixels of the order of a few percent are important, then these fluctuations have to be taken into account by using a different calibration constant for each pixel. Note that the number of electron–hole pairs created is proportional to the photon energy. This is reflected in the two different values of k, 0.682 and 0.792 at 6.93 and 8.05 keV, respectively.

The inset of Fig. 2 shows the autocorrelation function of $V(\boldsymbol{r},t)$ as calculated from Eq. (11) for nearest neighbor coupling ($\Delta = 1$). Here $\boldsymbol{r}$ has been replaced by an integer index for the one dimensional detector. The spatial average of the correlation function, $\langle C(i,1)\rangle_i = 0.2201 \pm 0.0004$. The spatial variance of the correlation function, $S^2_{i,C} = (1.21 \pm 0.06) \times 10^{-4}$, agrees well with the expected variance [13] of $1/N$, where N is the number of scans averaged. Within error, $C(i,1)$ is equal for all pixels. For larger Δ, we found $\langle C(i,2)\rangle_i = 0.0319$, $\langle C(i,3)\rangle_i = 0.0062$, $\langle C(i,4)\rangle_i = 0.0012$ and $\langle C(i,5)\rangle_i = 0.0004$, all measured within ± 0.0004. The technique is very sensitive, since we can measure very small correlations between pixels sepa-

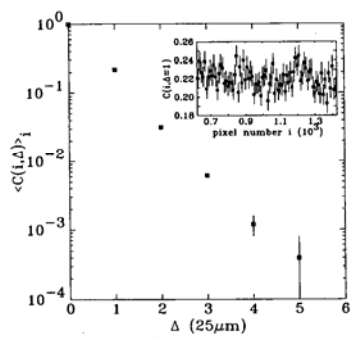

Fig. 2. Spatial average of $C(i,\Delta)$, as defined in Eq. (11), versus Δ. Each point was calculated from an average over all pixels of $C(i,\Delta)$, shown in the inset for $\Delta = 1$.

rated by 100 μm. Fig. 2 shows $\langle C(i,\Delta)\rangle_i$ versus Δ. The decay of the correlation function is approximately exponential, which is consistent with the diffusion of the electric charge to neighboring pixels [14].

As discussed in Section 2, the resolution function $h(i')$ is evaluated from Eqs. (13)–(15), based on the assumption that only $h(0)$, $h(-1)$ and $h(1)$ are non-zero, and that $h(-1) = h(1) = h_1$. Replacing the integrals by sums in Eqs. (13)–(15), one finds that

$$k = \frac{S_{i,V}^2}{\langle V\rangle_i} = \frac{(h_0^2 + 2h_1^2)}{(h_0 + 2h_1)} = 0.792, \tag{17}$$

and

$$\langle C(i,\Delta = 1)\rangle_i = \frac{(2h_0h_1)}{(h_0^2 + 2h_1^2)} = 0.2201, \tag{18}$$

which gives $h_0 = 0.947$ and $h_1 = 0.107$. To transform the signal V to detected photons, one must divide V by $\int h(r)\,\mathrm{d}r = h_0 + 2h_1 = 1.16$ instead of by k. The above model reproduces the essential features but does not give the next nearest neighbors correlation correctly. With this model, $\langle C(i,2)\rangle_i = h_1^2/(h_0^2 + 2h_1^2) = 0.012$, which is lower than the observed correlation. This can be fixed by extending the range of the response function to the third neighbor [15].

The detective quantum efficiency was evaluated by measuring n_i with a scintillation counter masked by a 1.3 mm hole, and then $\langle V\rangle_r$ was measured by centering the height of the PSD behind this hole. Using Eq. (16), we find $\alpha = 37 \pm 2\%$ for 8.05 keV X-rays. This can be compared to the expected detective quantum efficiency estimated for transmission through the 250 μm Be window of the detector, transmission through an additional 1 μm SiO_2 overcoat and the fraction of absorbed X-rays in the electron diffusion length of the Si, t_{Si},

$$\alpha = \exp(-\mu_{Be}\rho_{Be}t_{Be})\exp(-\mu_{SiO_2}\rho_{SiO_2}t_{SiO_2}) \times [1 - \exp(-\mu_{Si}\rho_{Si}t_{Si})]. \tag{19}$$

Using the mass absorption coefficients 1.1, 36.4, 64.7 cm^2/g for Be, Si and SiO_2, respectively [16] at 8.05 keV, and densities of 1.85, 2.32, 2.21 g/cm^3, and a diffusion length $t_{Si} = 50$ μm as specified by the manufacturer [17], this estimate gives $\alpha = 50\%$, and agrees reasonably well with the measured value.

4. Characterization of a CCD array

The principle of photon detection of a CCD is similar to the linear array described in Section 2. In a CCD, the detected charge is stored in MOS capacitors and read by a series of parallel row transfers and serial pixel-to-pixel transfers. For coherent X-ray experiments [4], we used a virtual phase architecture TI 4849 chip, with 390 × 584 22.4 μm wide square pixels. The depletion depth of the chip is 12 μm, which gives a sufficient detective quantum efficiency for direct X-ray illumination. Further detail is given in Table 2 and elsewhere [18–21]. To characterize the detector, measurements were made at the high brilliance wiggler beamline X25 at NSLS with a Si(111) monochromator set at 7.0 keV. Fig. 3 shows the experimental set up.

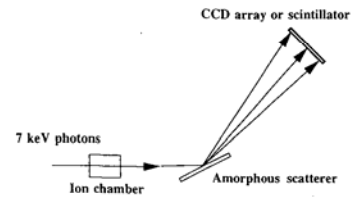

Fig. 3. Experimental set up for the characterization of the CCD array. The X-ray beam was scattered with a piece of polystyrene to produce a spatially uniform exposure [7,9]. The detector was centered at a scattering angle of $2\Theta = 23°$ and placed 1.04 m from the center of rotation. n_i could be varied by detuning the monochromator, and therefore modifying the incident flux, or by varying the integration time τ from 1 to 240 s. An ion chamber was used to monitor the incident intensity on the sample, and a scintillation detector, masked with a 4 mm circular aperture, was placed at the CCD position and allowed us to determine n_i. This way, the scintillator signal was used to calibrate the ion chamber signal (I_{mon}). Using the ratio of areas and counts, the count rate per pixel was obtained, based on I_{mon}. The highest count rate was 1 photon/(22.4 μm)^2/sec.

The ratio $k = S_{r,V}^2/\langle V\rangle_r$ is shown in Fig. 4 as a function of $\langle n_i\rangle_r$. For a detector with a linear response, k is a constant, independent of n_i. We were quite surprised to see a nonlinear relationship for k because the response to visible light had been measured to be linear to within 0.5% [18–21]. It was later discovered that an inappropriate amplifier was

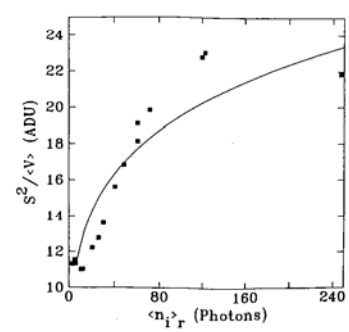

Fig. 4. $k = S_{r,V}^2/\langle V\rangle_r$ versus the incident integrated intensity on the detector $\langle n_i\rangle_r$. The average and variance were calculated over a region of 100 by 100 pixels. The solid line is a least squares fit.

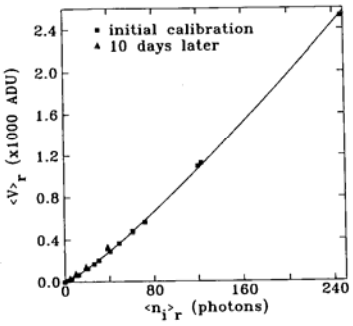

Fig. 5. Spatial average of the signal $V(r,t)$ over a region of 100 by 100 pixels versus the number of photons incident on the surface of a pixel $\langle n_i \rangle_r$. Two data sets taken ten days apart (squares and triangles) are shown. The solid line is a least squares fit to the first calibration with $n_i = 0.35V^{0.84}$. This function is applied to the measured signal to linearize it. V was less than 75% of the saturation value for all points.

responsible for the non-linearity. When recently tested with the correct operating electronics, the response to X-rays was linear. Since the model used in Section 2 assumes linearity, it will be generalized below to include a non-linear response.

4.1. A treatment for a non-linear detector

In many X-ray scattering experiments, one needs to determine n_i instead of n_d. This is done by calibrating the response of the PSD, V, for different n_i. Fig. 5 shows the mean of the CCD response over a region of 100×100 pixels, $\langle V \rangle_r$, versus n_i. The calibration was checked ten days later and remained mostly unchanged. The response of the detector depends only on n_i, since all the data points with an equal integrated flux $I_{\text{mon}}\tau$ fall on the same line in Fig. 5 although they differ widely in exposure times and incident flux. Several functions were tried to obtain an analytic relation for the CCD response. The solid line in Fig. 5, $n_i = f^{-1}(V) = 0.35V^{0.84}$, is the best least squares fit found. This function allows one to linearize the measured signal V with sufficient accuracy.

The linearized signal, v^*, is defined by $v^* = f^{-1}(V)$. It has the same units as n_i, but its statistics is different from the Poisson statistics of n_i. In order to determine the noise in the linearized signal, we evaluated the spatial variance of v^*, S^2_{r,v^*}, in a region of 100×100 pixels versus n_i (see Fig. 6). The solid line is the relation expected for a Poisson distribution ($S^2_{r,v^*} = \langle n_i \rangle_r$), while the dotted line is $S^2_{r,v^*} = 1.63\langle n_i \rangle_r$. The variance is larger because the spatial resolution of the CCD is larger than the area of a pixel, and α is smaller than one.

Fig. 7 shows averages of a single exposure of $V(r,t)$ taken over columns and rows of the detector. Pixels which

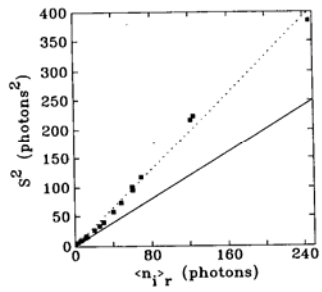

Fig. 6. The spatial variance of the linearized data measured in a region of 100 by 100 pixels versus the linearized signal. One would expect the variance S^2_{r,v^*} to go as $\langle n_i \rangle_r$ in the case of a simple Poisson law (solid line). The dotted line is $1.63\langle n_i \rangle_r$.

are in the rows 110 to 480 and columns 10 to 380, which represent most of the detector area, are used for the averages. The mean is uniform in both directions with rms fluctuations of 2%. Fig. 8 shows a bitmap of the variance $S^2_{t,V}$, calculated from 23 frames, each exposed for 1 s. The variance is uniform over the whole detector area, except for a few bad columns in the parallel transfer direction (y-axis), where the variance is significantly lower. Pixels in columns 26–28, 72–73, 181–182, 208–209, have 40 to 80% less than average variance. This is shown in Fig. 9, where the average of $S^2_{t,V}$ over row 420 to 520 is displayed as a function of the horizontal position. A similar average of $\langle V \rangle_t$ is shown for comparison. The mean only fluctuates by a few percent. It is important to measure the noise of each pixel to fully characterize the detector.

The resolution function is extracted from the spatial cor-

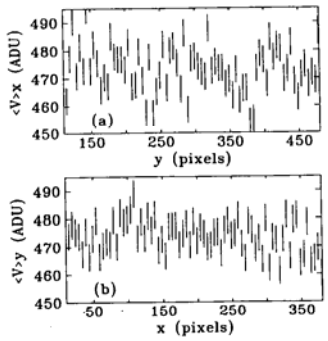

Fig. 7. (a) Signals summed over 370 rows (top) and 370 columns.

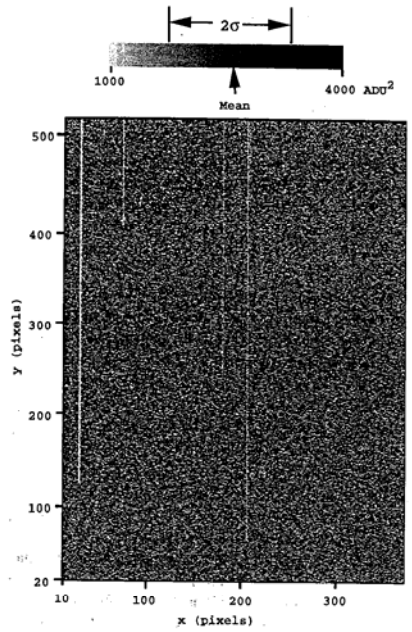

Fig. 8. Time averaged variance $S^2_{t,V}(\boldsymbol{r})$ of the pixels in row 20 to 520 and column 10 to 380. 23 exposures of one seconds each were averaged. An inverted grey scale is used to display the data. On the top scale, the spatial average and the standard deviation of $S^2_{t,V}(\boldsymbol{r})$ are marked. Note that the variance is relatively uniform except for pixels in certain columns, where the variance is much lower.

relation $C(\boldsymbol{\Delta})$, defined by

$$C(\boldsymbol{\Delta}) = \frac{\langle (v^*(\boldsymbol{r},t)v^*(\boldsymbol{r}+\boldsymbol{\Delta},t))_r - \langle (v^*(\boldsymbol{r},t))_r^2}{S^2_{r,v^*}(t)}, \tag{20}$$

where the displacement $\boldsymbol{\Delta}$ is measured in units of pixels. This definition is similar to Eq. (11). Sufficiently good statistics can be achieved based on a single exposure of the CCD. A fast calculation algorithm may be used [22]. Knowledge of $C(\boldsymbol{\Delta})$ is necessary for coherent X-ray experiments, where one is interested in the speckle size, which is of the order of the pixel dimensions [4]. Fig. 10 shows two slices of $C(\Delta x, \Delta y)$, where the first index refers to the columns and the second to the rows of the CCD array. The correlation function $C(\Delta, 0)$ decays more slowly than $C(0, \Delta)$, i.e. the resolution is worse along the serial transfer direction than along the parallel transfer direction. The correlation coefficients are non-zero for the nearest and next nearest neighbor of $C(0,0)$, with $C(1,0) = 0.52 \pm 0.05$, $C(0,1) = 0.12 \pm 0.01$ and $C(1,1) = C(-1,1) = 0.07 \pm 0.02$. Note that $C(\boldsymbol{\Delta}) = C(-\boldsymbol{\Delta})$, based on Eq. (20). Thus the resolution function has a range of one to two pixels. Using the simplest model, we choose $h(\boldsymbol{r})$ to be non zero only for the nearest neighbors, i.e. $h(0,0) = h_{00}$, $h(1,0) = h(-1,0) = h_{10}$ and $h(0,1) = h(0,-1) = h_{01}$. We choose to normalize the integral of $h(\boldsymbol{r})$ to unity, assuming that one photon will

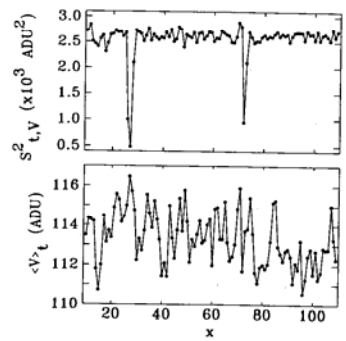

Fig. 9. Average of $S^2_{t,V}(\boldsymbol{r})$, calculated over a column between row 420 and 520 of the CCD, shown versus the index of the column. The pixels in columns 26 to 28 and 72 to 73, have much lower variance than other pixels. $\langle V \rangle_t$ is shown for comparison. The mean shows typical behavior for these columns. It is important to measure the variance of the signal of each pixel when one performs intensity fluctuation spectroscopy with a CCD.

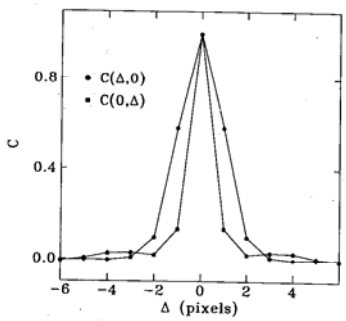

Fig. 10. Two perpendicular slices of the space autocorrelation function, defined by Eq. (20), for uniform scattering data. $C(\Delta, 0)$ for the serial transfer direction (circles) and $C(0, \Delta)$ for the parallel transfer direction (squares) are shown versus Δ. The error bars are slightly larger than the size of the squares. The correlation decays to 0 in about two pixels along x, the serial transfer direction, and in one pixel perpendicular to it.

be distributed amongst several pixels so that

$$h_{00} + 2h_{10} + 2h_{01} = 1. \tag{21}$$

From Eq. (15), the correlation function of this disturbance gives

$$C(1,0) = \frac{2h_{00}h_{10}}{h_{00}^2 + 2h_{10}^2 + 2h_{01}^2} = 0.52, \tag{22}$$

and

$$C(0,1) = \frac{2h_{00}h_{01}}{h_{00}^2 + 2h_{10}^2 + 2h_{01}^2} = 0.12. \tag{23}$$

Solving Eqs. (21)–(23), we find $h_{00} = 0.563, h_{01} = 0.042, h_{10} = 0.177$. A larger fraction of the signal leaks to the nearest neighbors along the serial transfer direction.

The resolution function alters the variance of the number of detected photons. From Eqs. (13) and (14), one finds

$$K_s \equiv \frac{S_{r,n_d}^2}{\langle n_d \rangle_r} = h_{00}^2 + 2h_{10}^2 + 2h_{01}^2 = 0.38. \tag{24}$$

Without leakage, $K_s = 1$, so that the variance is smaller than what one expects from Poisson noise by a factor K_s. Using $\langle n_d(\boldsymbol{r}) \rangle_r = \alpha \langle v^*(\boldsymbol{r}) \rangle_r$, assuming that α is the same for each pixels, one gets

$$S_{r,n_d}^2 = \alpha^2 S_{r,v^*}^2 = K_s \alpha \langle v^* \rangle_r. \tag{25}$$

From a Taylor's expansion of the linearization function, $v^* = f^{-1}(V)$, one obtains

$$S_{r,v^*}^2 = S_{r,V}^2 (\mathrm{d}v^*/\mathrm{d}V)^2, \tag{26}$$

where S_{r,v^*}^2 is the variance of the linearized data. Recalling that for the linearization function, $\mathrm{d}v^*/\mathrm{d}V = B\langle v^* \rangle_r / \langle V \rangle_r$ and substituting Eq. (26) into Eq. (25), one gets

$$\frac{S_{r,V}^2}{\langle V \rangle_r} = \frac{K_s \langle v^* \rangle_r}{\alpha \langle V \rangle_r (\mathrm{d}v^*/\mathrm{d}V)^2} = \frac{K_s \langle V \rangle_r}{\alpha \langle v^* \rangle_r B^2}, \tag{27}$$

where B is the exponent of the power law fit in Fig. 5 equal to 0.84. This equations includes three different contributions in the ratio: the smearing from the finite resolution, the non-linear behavior and the detective quantum efficiency. For a linear detector ($B = 1$), with a resolution of one pixel area ($K_s = 1$), Eq. (27) becomes equivalent to Eq. (6). Therefore $S_{r,V}^2/\langle V \rangle_r$ is not constant (see Fig. 4), since $\langle V \rangle_r / \langle n_i \rangle_r$ is non-linear. Fitting the measured CCD response in Fig. 4 to Eq. (27) gives a detective quantum efficiency $\alpha = 0.22$. Eq. (19), with the values $\mu_{Si} = 94.9\ \mathrm{cm^2/g}$, $\mu_{Be} = 1.6\ \mathrm{cm^2/g}$ [16], $t_{SiO_2} = 0\ \mu\mathrm{m}$ and $t_{Si} = 12\ \mu\mathrm{m}$, gives $\alpha = 0.22$, which agrees well with the measurement. Furthermore, Eq. (25) gives $K_s/\alpha = 1.5$, which corresponds to the ratio of $S_{r,v^*}^2/\langle v^* \rangle_r$ in Fig. 6.

5. Conclusion

One must carefully characterize the response of a current state-of-the-art PSD to obtain quantitative information. For example, in our intensity fluctuation spectroscopy experiments, it is essential to distinguish the noise of the detector from measured scattered intensity fluctuations, and we must know the spatial correlations of the detector's resolution function quite accurately. We have shown that we can characterize a PSD by measuring means, variances, and spatial autocorrelation functions and comparing these measurements to the statistical estimators expected for a Poisson distribution. The technique can measure the resolution function, and gives an estimate of the detective quantum efficiency. It is easy to implement and can be very sensitive when enough scans are averaged. The mean and variance arrays are easily calculable in real time by storing only three arrays in memory [23]. The technique can also handle detector non-linearities. A simple extension of the technique would be to measure the decay of the time correlation function of the CCD signal, when the detector is optically coupled to a X-ray fluorescent material. The advantage of using the correlation function here is that no special hardware, such as a fast shutter, is required for the experiment.

Acknowledgments

We wish to thank Claude Lacoursière, William Leo and Roy Frieden for useful comments on statistics and error analysis. This work was supported by the Natural Sciences and Engineering Council of Canada, le Fonds pour la Formation des Chercheurs et l'Aide à la Recherche du Québec, and by the US Department of Energy, BES-Materials Science, under grant contract No. W-31-109-ENG-38. This research was carried out in part at the National Synchrotron Light Source, Brookhaven National Laboratory, which is supported by the U.S. Department of Energy, Division of Materials Science and Division of Chemical Sciences.

Appendix A

One often wants to evaluate the uncertainty in the estimated average $\langle x \rangle$ and variance S^2 of a random variable X, with theoretical mean μ and variance σ^2. Assuming that the probability density $\rho(x)$ of the random variable X is stationary, the true mean and variance of $\rho(x)$ are defined by

$$\overline{x} = \int_{-\infty}^{\infty} x\rho(x)\ \mathrm{d}x = \mu \tag{A.1}$$

and

$$\overline{(x-\mu)^2} = \int_{-\infty}^{\infty} (x-\mu)^2 \rho(x)\ \mathrm{d}x = \sigma^2, \tag{A.2}$$

with $\int_{-\infty}^{\infty} \rho(x)\ \mathrm{d}x = 1$. The discussion below is limited to distributions with finite μ and σ^2. The statistical estimators of the mean $\langle x \rangle$ and variance S^2 are defined by

$$\langle x \rangle = \frac{1}{N} \sum_{i=1}^{N} x_i, \tag{A.3}$$

and

$$S^2 = \frac{1}{N-1} \sum_{i=1}^{N} (x_i - \langle x \rangle)^2, \tag{A.4}$$

where x_i is a measured outcome of the random variable X, chosen from the same probability distribution $\rho(x)$. The estimators $\langle x \rangle$ and S^2 are unbiased estimators of the mean and variance and on average are equal to μ and σ^2. The uncertainties in these statistical estimators depend on the number of random events observed, N. For small N, the fluctuations in the measured or estimated value are comparable to the expected value. Therefore, its dependence on N must be well characterized.

The uncertainty on the mean is well known and goes as $\sqrt{\sigma^2/N}$ [11]. For a Gaussian distribution, the uncertainty on the variance is $\sqrt{2/(N-1)}\sigma^2$ [11]. In Section A.1, we derive a general relation for the uncertainty of the estimated variance, and apply it to the Poisson distribution. In error propagation analysis, one may want to evaluate the uncertainty in a function of the mean and variance $f(\langle x \rangle, S^2)$ as required in Section 2. To evaluate the error in f, one uses the uncertainty on $\langle x \rangle$ and S^2, and needs to know the covariance between $\langle x \rangle$ and S^2. A general expression for this covariance is derived in Section A.2, and a derivation for Eq. (7) is shown in Sections A.3 and A.4.

A.1. Uncertainty in the measured mean and variance

It is important to note that $\langle x \rangle$ and S^2 are themselves random variables since they are functions of several random variables. A useful estimator of the uncertainty of these new random variables is their standard deviations $\sigma_{\langle x \rangle}$ and σ_{S^2} defined in Ref. [11] by

$$\sigma^2_{\langle x \rangle} = \overline{\langle x \rangle^2} - \overline{\langle x \rangle}^2, \tag{A.5}$$

and

$$\sigma^2_{S^2} = \overline{S^4} - \overline{S^2}^2, \tag{A.6}$$

where the horizontal line refers to an average over the joint probability distribution of the random variable $\langle x \rangle$, a function of N random variables x_i, i.e.

$$\overline{\langle x \rangle} \equiv \int \langle x \rangle (x_1, \ldots, x_N) \rho(x_1, \ldots, x_N)\ \mathrm{d}x_1 \ldots \mathrm{d}x_N.$$

$\sigma_{\langle x \rangle}$ and σ_{S^2} are the standard deviations of the probability densities of $\langle x \rangle$ and S^2. The N dependence in Eqs. (A.5) and (A.6) is not explicitly written in order to keep the notation simple. From Eq. (A.3), recalling that $\overline{x_i} = \mu$, it is easy to show that $\overline{\langle x \rangle} = \mu$. In order to simplify the algebra below, we introduce a new variable $y_i = x_i - \mu$, so that $\overline{y_i} = 0$ and $\overline{y_i^2} = \sigma^2$. One can now rewrite Eq. (A.5), using Eq. (A.3) and square it to get

$$\sigma^2_{\langle x \rangle} = \frac{1}{N^2} \sum_{i,j=1}^{N} \overline{y_i y_j}. \tag{A.7}$$

Assuming that each y_i is independent, i.e.

$$\overline{y_i y_j} = \delta_{ij} \sigma^2, \tag{A.8}$$

where δ_{ij} is a Kronecker delta, and replacing Eq. (A.8) in Eq. (A.7), one gets

$$\sigma^2_{\langle x \rangle} = \frac{\sigma^2}{N}, \tag{A.9}$$

which is a well known result valid for any N, and any probability distribution with finite mean and variance, given that no correlation exists between the x_i's. This result states that the probability density of $\langle x \rangle$, $\rho(\langle x \rangle)$, is narrower than $\rho(x)$ by a factor $\sqrt{1/N}$.

In Eq. (A.6), the $\overline{S^2}$ term can be evaluated by substituting x_i by y_i and replacing Eq. (A.3) into Eq. (A.4). Then, one finds

$$S^2 = \frac{1}{N-1} \left(\sum_{i=1}^{N} y_i^2 - \frac{1}{N} \sum_{i,j=1}^{N} y_i y_j \right). \tag{A.10}$$

Taking averages on both sides of Eq. (A.10), and evaluating the sums with Eq. (A.8), one finds $\overline{S^2} = \sigma^2$, as stated before. The $N-1$ denominator comes from the fact that there is one less degree of freedom used to evaluate the mean. Taking the square of Eq. (A.10), and taking averages on the right and left hand side of the equation, one finds

$$\overline{S^4} = \frac{1}{(N-1)^2} \left(\sum_{i,j=1}^{N} \overline{y_i^2 y_j^2} - \frac{2}{N} \sum_{i,j,k=1}^{N} \overline{y_i^2 y_j y_k} + \frac{1}{N^2} \sum_{i,j,k,l=1}^{N} \overline{y_i y_j y_k y_l} \right). \tag{A.11}$$

Evaluating the averages recalling that $\overline{y_i} = 0$ and $\overline{y_i y_j} = \delta_{ij}\sigma^2$, one finds

$$\overline{y_i^2 y_j^2} = \begin{cases} \overline{y^4}, & \text{for } i = j,\ N \text{ terms}, \\ \sigma^4, & \text{for } i \neq j,\ N(N-1) \text{ terms}, \end{cases} \tag{A.12}$$

$$\overline{y_i^2 y_j y_k} = \begin{cases} \overline{y^4}, & \text{for } i = j = k,\ N \text{ terms}, \\ \sigma^4, & \text{for } i \neq j = k,\ N(N-1) \text{ terms}, \\ 0, & \text{otherwise}, \end{cases}$$

$$\overline{y_i y_j y_k y_l} = \begin{cases} \overline{y^4}, & \text{for } i=j=k=l,\ N \text{ terms}, \\ \sigma^4, & \text{for } i=j \neq k=l,\ 3N(N-1) \text{ terms}, \\ 0, & \text{otherwise}. \end{cases} \tag{A.14}$$

Here, the nth order central moment is defined by $\overline{y^n} \equiv \int y^n \rho(y)\, dy$. Using Eqs. (A.12)–(A.14) to evaluate the sums in Eq. (A.11), and replacing Eq. (A.11) into Eq. (A.6), one finds

$$\sigma^2_{S^2} = \frac{\overline{y^4}(N-1) + \sigma^4(3-N)}{N(N-1)}. \tag{A.15}$$

This result depends on the fourth order central moment of the distribution, $\overline{y^4}$, and the standard deviation, σ. For a Gaussian distribution, $\overline{y^4} = 3\sigma^4$ [10] and Eq. (A.15) gives as expected that, $\sigma^2_{S^2} = 2\sigma^4/(N-1)$. For a Poisson distribution on the other hand, $\overline{y^4} = 3\mu^2 + \mu$ [10] which yields

$$\sigma^2_{S^2} = \frac{2}{N-1}\mu^2 + \frac{\mu}{N}. \tag{A.16}$$

Note that for $\mu < 1$, the second term is an important correction and a Gaussian approximation would underestimate the error on the variance. For large means, Eq. (A.16) becomes identical to the error for a Gaussian with variance equal to the mean, as expected since the Poisson distribution crosses over to such a Gaussian for large means. Finally, note that since in general $\rho(S^2)$ is not Gaussian, one cannot easily quantify the confidence limits of S^2, but can nevertheless calculate its variance.

A.2. Correlation of the sample mean and variance

One might think that there is no correlation between the estimator of the mean $\langle x \rangle$ and the estimator of the variance S^2. The independence of the estimated mean and variance is discussed in several statistical books for Gaussian distributions [8,11]. The measure of correlation between the measured mean and variance, the covariance, is defined as

$$\begin{aligned} &\mathrm{cov}(\langle x \rangle, S^2) \\ &= \overline{(\langle x \rangle - \mu)(S^2 - \sigma^2)} = \overline{\langle y \rangle S^2} \\ &= \frac{1}{N(N-1)} \left(\sum_{i,j=1}^{N} \overline{y_i y_j^2} - \frac{1}{N} \sum_{i,j,k=1}^{N} \overline{y_i y_j y_k} \right), \end{aligned} \tag{A.17}$$

since $\overline{\langle y \rangle \sigma^2} = 0$. Evaluating the averages as in Eqs. (A.12)–(A.14), one finds

$$\overline{y_i y_j y_k} = \begin{cases} \overline{y^3}, & \text{for } i=j=k,\ N \text{ terms}, \\ 0, & \text{otherwise}. \end{cases} \tag{A.18}$$

The same results holds for $\overline{y_i y_j^2}$. Replacing those in Eq. (A.17) and simplifying, one gets

$$\mathrm{cov}(\langle x \rangle, S^2) = \frac{\overline{y^3}}{N}, \tag{A.19}$$

where $\overline{y^3}$ is the 3rd order central moment of the distribution. Thus the covariance depends on N, and on how symmetric with respect to the mean is the probability distributed. The estimated mean and variance are independent only as N goes to infinity, or if $\overline{y^3} = 0$. For a Gaussian distribution, the covariance is zero because odd powers of the central moments are zero. For a Poisson distribution, $\overline{y^3} = \mu$ [10] and

$$\mathrm{cov}(\langle x \rangle, S^2) = \frac{\mu}{N}. \tag{A.20}$$

A.3. Evaluation of the error on a function of S^2 and $\langle x \rangle$

From standard error propagation analysis [8], one can readily calculate the uncertainty of a function $f(\langle x \rangle, S^2) = S^2/\langle x \rangle$. It is given by

$$\frac{\sigma_f^2}{f^2} \approx \frac{\sigma^2_{S^2}}{\overline{S^2}^2} + \frac{\sigma^2_{\langle x \rangle}}{\overline{\langle x \rangle}^2} - \frac{2\,\mathrm{cov}(S^2, \langle x \rangle)}{\overline{\langle x \rangle S^2}}, \tag{A.21}$$

where the terms on the right hand side have been calculated above. The approximate sign comes from the fact that σ_f is derived from a first order Taylor expansion of f around its average. Replacing the uncertainties and covariance derived previously for a Poisson distributed random variable X in Eqs. (A.9), (A.16) and (A.20), one finds

$$\frac{\sigma_f^2}{f^2} \approx \frac{2}{N-1}. \tag{A.22}$$

The result is independent of the mean μ and by averaging N independent measurements, one can measure f accurately. On the other hand, if the signal is Gaussian distributed, the covariance term in Eq. (A.21) would be zero, and one gets

$$\frac{\sigma_f^2}{f^2} \approx \frac{2}{N-1} + \frac{\sigma^2}{\mu^2 N}.$$

Depending on the mean and variance of the distribution, the second term may be important.

A.4. Including electronic noise for an X-ray detector

For an X-ray detector, Eq. (A.22) is not sufficient to estimate the errors on k, defined in Eq. (5), because for weak signals, the electronic noise will contribute significantly to σ_k. V_e, the dark electronic noise, increases the relative error on the time averaged mean $\langle V \rangle_t$ and variance $S^2_{t,V}$ when the contribution from the detected photons approaches zero. To find σ_k, the standard deviation of k, we can simply replace in Eq. (A.21) $\langle x \rangle$ by $\langle V \rangle_t$, and S^2 by $S^2_{t,V} - \sigma^2_{V_e}$, where $\sigma^2_{V_e}$

is the theoretical variance of the electronic noise probability distribution. Then the first term of Eq. (A.21) can be rewritten as

$$\frac{\sigma^2_{S^2_{r,V}-\sigma^2_{V_e}}}{(\overline{S^2_{r,V}}-\sigma^2_{V_e})^2} = \frac{\sigma^2_{k^2 S^2_{n_d}} + \sigma^2_{S^2_{V_e}}}{(\overline{S^2_{r,V}}-\sigma^2_{V_e})^2} = \frac{2}{N-1} + \frac{1}{Nn_d} + \frac{2\sigma^4_{V_e}}{(N-1)(\overline{S^2_{r,V}}-\sigma^2_{V_e})^2}. \quad (A.23)$$

To obtain this relationship, we used the equation $\sigma^2_{S^2_{r,V}-\sigma^2_{V_e}} = \sigma^2_{S^2_{r,V}}$ and Eq. (3), and assumed that V_e follows Gaussian statistics. The first two terms are the detected photon contributions which are included in Eq. (A.22), and the last term is due to an error on the evaluation of the dark variance. Next, we can evaluate the second term of Eq. (A.21) using Eq. (3),

$$\frac{\sigma^2_{\langle V\rangle_r}}{\overline{\langle V\rangle_r}^2} = \frac{k^2\sigma^2_{n_d} + \sigma^2_{V_e}}{N\overline{\langle V\rangle_r}^2} + \frac{\sigma^2_{V_e}}{N_d\overline{\langle V\rangle_r}^2} = \frac{1}{Nn_d} + \frac{\sigma^2_{V_e}}{\overline{\langle V\rangle_r}^2}\left(\frac{1}{N}+\frac{1}{N_d}\right), \quad (A.24)$$

where n_d and $\overline{\langle V\rangle_r}$ are the hypothesized means of the number of detected photons and of the detector signal, while $\sigma^2_{n_d}$ and $\sigma^2_{V_e}$ are the theoretical variances of n_d and of the dark electronic noise. The first term in this equation comes from the statistics of the detected photons and is already included in Eq. (A.22). The second term explains the increased uncertainty in k for small signals due to the electronic noise. The third term is due to the statistical error in the measurement of the dark pattern subtracted from V, where N_d scans are averaged without X-rays. To minimize the error, one should choose $N_d = N$. Finally, the last term in Eq. (A.21) is unchanged from the Poisson case because the dark signal and the detected photon signal are not correlated. Collecting terms, we find

$$\frac{\sigma^2_k}{k^2} \approx \frac{2}{N-1}\left(1+\frac{\sigma^4_{V_e}}{(\overline{S^2_{r,V}}-\sigma^2_{V_e})^2}\right) + \frac{\sigma^2_{V_e}}{\overline{\langle V\rangle_r}^2}\left(\frac{1}{N}+\frac{1}{N_d}\right). \quad (A.25)$$

It is therefore easier to measure k when $\langle V\rangle_r^2$ and $S^2_{r,V}$ are much larger than $\sigma^2_{V_e}$. To evaluate σ_k for a given experiment, one would replace $\sigma^2_{V_e}$, $\overline{S^2_{r,V}}$ and $\overline{\langle V\rangle_r}$ by the experimentally measured values S^2_{r,V_e}, $S^2_{r,V}$ and $\langle V\rangle_r$.

Note that the error analysis approach developed above can be extended to other problems, like the evaluation of the error on the measured contrast in optics if the signal is not Gaussian distributed. It is also useful to estimate the errors in our coherent X-ray experiments.

References

[1] S. Brauer, J.O. Ström-Olsen, M. Sutton, Y.S. Yang, A. Zaluska, G.B. Stephenson and U. Köster, Phys. Rev. B 45 (1992) 7704.

[2] B. Park, G.B. Stephenson, S.M. Allen, K.F. Ludwig Jr., Phys. Rev. Lett. 68 (1992) 1742.

[3] K.F. Ludwig Jr., G.B. Stephenson, J.L. Jordan-Sweet, J. Mainville, Y.S. Yang and M. Sutton, Phys. Rev. Lett. 61 (1988) 1859.

[4] M. Sutton, S.G.J. Mochrie, T. Greytak, S.E. Nagler, L.E. Berman, G.A. Held and G.B Stephenson, Nature 352 (1991) 608; M. Sutton, E. Dufresne, S.G.J. Mochrie, L.E. Berman, G.A. Held and G.B Stephenson, in: NSLS Annual Report (BNL 52317 1991) p. 293. E. Dufresne, R. Brüning, M. Sutton, G.B Stephenson, B.G. Rodricks, C. Thompson and S.E. Nagler in: NSLS Annual Report (BNL 52371 1993) p. 381.

[5] R. Clarke, W. Dos Passos, W. Lowe, B.G. Rodricks and C. Brizard, Phys. Rev. Lett. 66 (1991) 317.

[6] S.S. Vogt, R.G. Tull, and P. Kelton, Appl. Optics, 17, (1978) 574; R.C. Jones, Adv. Electron. Electron. Phys. 11 (1959) 87.

[7] G.B. Stephenson, in: Early-Stage Phase Separation in Amorphous Solids: A Time Resolved SAX Study (Stanford Synchrotron Radiation Laboratory, Report 82/05 1982) p. 140; J.R. Janesick, K.P. Klaasen and T. Elliott, Opt. Engng. 26 (1987) 972.

[8] W.R. Leo, in: Techniques for Nuclear and Particle Physics Experiments, (Springer, New York, 1987) pp. 83–106, 220.

[9] J. Mainville, Ph.D. Thesis, McGill University (1992).

[10] A Poisson distribution is discrete. The probability of measuring n events is $P(n) = \mu^n e^{-\mu}/n!$. The mean and the variance are μ. Higher central moments are $\overline{(x-\mu)^3} = \mu$, and $\overline{(x-\mu)^4} = 3\mu^2+\mu$. A Gaussian distribution is continuous, with probability density $\rho(x) = 1/\sqrt{2\pi}\sigma \exp[(x-\mu)^2/2\sigma^2]$. The mean is μ and the variance is σ^2. Higher moments are $\overline{(x-\mu)^3} = 0$ and $\overline{(x-\mu)^4} = 3\sigma^4$.

[11] B.R. Frieden, in: Probability, Statistical Optics and Data Testing, 2nd ed. (Springer, New York, 1991) pp. 218–228, 234–248.

[12] In a real PSD, h may depend on where the photon is absorbed on the area of the pixel, and on how deep it is absorbed. Furthermore, the probability for a photon of being absorbed varies exponentially with depth. Here we assume the response h independent of the exact position of the photon absorption. This is the simplest model for describing the spread of the signal to several pixels. It could be generalized in a straightforward manner.

[13] W.H. Press, S.A. Teukolsky, W.T. Vetterling and B.P. Flannery, in: Numerical Recipes in C, 2nd Edition (Cambridge Univ. Press, Cambridge, 1992) p. 636.

[14] L.N. Koppel, Adv. X-ray Anal. 19 (1976) 587.

[15] The simplest model fitting all data points requires four parameters. By including h_2 and h_3 in the model, we can solve simultaneously the equations for the ratio and for the five correlation functions using a non-linear least squares fit program. Eq. (17) becomes

$$k = \frac{S^2_{r,V}}{\langle V\rangle_r} = \frac{h_0^2+2h_1^2+2h_2^2+2h_3^2}{h_0+2h_1+2h_2+2h_3} = 0.792,$$

Eq. (18) is rewritten

$$\langle C(i,\Delta=1)\rangle_i = \frac{2h_0h_1+2h_1h_2+2h_2h_3}{h_0^2+2h_1^2+2h_2^2+2h_3^2} = 0.2201,$$

and so on. One then finds $h_0 = 0.964$, $h_1 = 0.108$, $h_2 = 0.0095$ and $h_3 = 0.002$.

[16] Nuclear Data Center, online database at Brookhaven National Laboratory. Telnet to bnlnd2.dne.bnl.gov, username nndc, search the X-ray absorption database.

[17] Technical information sheet on the RL2048S Solid State Line Scanner 2048 elements, EG&G Reticon, 345 Potrero Avenue, Sunnyvale, California 94086-4197.

[18] B. Rodricks and C. Brizard, Nucl. Instr. and Meth. A 311 (1992) 613.

[19] C. Brizard and B. Rodricks, Rev. Sci. Instr. 63 (1992) 803.

[20] R. Clarke, B. Rodricks and R. Smither, Rev. Sci. Instr. 60 (1989) 2280.

[21] B. Rodricks, R. Clarke, R. Smither and A. Fontaine, Rev. Sci. Instr. 60 (1989) 2586.

[22] We use a standard fast Fourier transform (fft) algorithm to calculate the spatial autocorrelation function, described in Ref. [13], Chapter 12. $C(\Delta) = \mathrm{fft}^{-1}(\mathrm{fft}(v^*)\mathrm{fft}^*(v^*))$, where $\mathrm{fft}(v^*)$ is the complex fft of v^*.

[23] Only three arrays are required. Storing the first pattern as an offset array $V(t_0)$, we store in two arrays the difference $A_1 = \sum_{i=0}^{i=N}(V(t_i) - V(t_0))$ and the square of the difference $A_2 = \sum_{i=0}^{i=N}(V(t_i) - V(t_0))^2$. Then, the mean $\langle V\rangle_t = A_1/N + V(t_0)$ and the variance $S^2_{t,V} = (A_2 - A_1^2/N)/(N-1)$. This algorithm minimizes the roundoff error (see Ref. [13] p. 613), and minimizes the disk space required for the calibration. Similar sums can be taken for calculating the correlation function in Eq. (11).